

See discussions, stats, and author profiles for this publication at: <https://www.researchgate.net/publication/252277018>

# Structural Aspects of the Swelling of $\beta$ Chitin in HCl and its Conversion into $\alpha$ Chitin

ARTICLE *in* MACROMOLECULES · JUNE 1997

Impact Factor: 5.8 · DOI: 10.1021/ma961787+

---

CITATIONS

58

---

READS

49

5 AUTHORS, INCLUDING:



Jean-Luc Putaux

French National Centre for Scientific Research

178 PUBLICATIONS 5,168 CITATIONS

SEE PROFILE



Françoise Gaill,

French National Centre for Scientific Research

201 PUBLICATIONS 3,544 CITATIONS

SEE PROFILE

## Structural Aspects of the Swelling of $\beta$ Chitin in HCl and its Conversion into $\alpha$ Chitin

Y. Saito,<sup>†</sup> J.-L. Putaux,<sup>†</sup> T. Okano,<sup>‡</sup> F. Gaill,<sup>§</sup> and H. Chanzy\*,<sup>†</sup>

Centre de Recherches sur les Macromolécules Végétales, CNRS, BP 53, 38041 Grenoble Cédex 9, affiliated with the Joseph Fourier University of Grenoble, France, Laboratory of Structural Biopolymers, Department of Biomaterial Sciences, Graduate School of Agriculture and Life Sciences, The University of Tokyo, Yayoi 1-1-1, Bunkyo-ku, Tokyo 113, Japan, and INSU CNRS Roscoff, URM7 IFREMER, Université Pierre et Marie Curie, 7 Quai Saint Bernard, 75252 Paris, Cédex 05, France

Received December 5, 1996; Revised Manuscript Received March 20, 1997<sup>®</sup>

**ABSTRACT:** The solid state transformation of chitin  $\beta$  into chitin  $\alpha$  under the influence of aqueous HCl of increasing concentration was investigated in the case of highly crystalline  $\beta$  chitin microfibrils isolated from the vestimentiferan tube of *Tevnia jerichonana*. With acid strength below 6 N, the chitin microfibrils remained un-affected. With acid strength between 6 and 7 N a total decrystallization was observed when the samples were immersed in the acid solution. When the initial  $\beta$  chitin was washed, crystals or one of their hydrates was restored, but the initially large microfibrils of chitin became split into a series of parallel subfibrils of much smaller diameter. With acid strength from 7 N to 8 N, decrystallization was also observed but it was accompanied by a substantial cutting and dissolution of the chitin chains. These smaller chains recrystallized in epitaxy on the remaining  $\beta$  chitin microfibrils in a subsequent washing step. In this case, the recrystallization led to morphologies resembling those of shish kebab where the "kebab" overgrowths consisted of  $\alpha$  chitin spindle-like crystals organized in epitaxy on the underlying  $\beta$  chitin microfibrillar remainder. When acid strengths of 8 N and above were used, the sample recrystallized exclusively as  $\alpha$  chitin upon washing. As opposed to the case where lower acid concentration was used, a total loss of the fibrillar morphology was observed with HCl of 8 N and above.

### Introduction

Chitin, the most abundant natural polymer after cellulose, is chiefly found as a fibrillar crystalline material. On the basis of infrared spectroscopy, as well as diffraction data, one distinguishes essentially two allomorphs of chitin, namely  $\alpha$  chitin which is the most abundant and  $\beta$  chitin which occurs more rarely.<sup>1–3</sup> The crystallography of both chitin allomorphs has been established by several authors. From their studies, it seems well established that  $\alpha$  chitin has a two chain unit cell with a  $P2_12_12_1$  space group and consequently an antiparallel arrangement of the chitin chains within each crystalline domain.<sup>4–6</sup> In  $\beta$  chitin crystals, the polymer chains are packed in a monoclinic  $P2_1$  space group with the chitin chain axis as the unique monoclinic axis. In this allomorph, there is only one chitin chain per unit cell. Therefore  $\beta$  chitin consists of a parallel chain arrangement.<sup>7–10</sup>

Upon dissolution or extensive intracrystalline swelling,  $\beta$  chitin converts itself invariably into  $\alpha$  chitin,<sup>4,11,12</sup> but it is not possible to go back to the  $\beta$  structure once the  $\alpha$  form has been reached. Thus,  $\beta$  chitin is considered as being a unique metastable entity resulting from a specific biosynthetic mechanism that must be different from the one leading to  $\alpha$  chitin. In fact some ultrastructural observations on the biogenesis of large whisker-like crystals of  $\beta$  chitin have been made. These observations indicate that the crystalline microfibrils of this allomorph originate from cup-shaped synthesizing organelles located in the plasma membranes of the corresponding organisms. In these organelles, a continuous biosynthesis coupled with unidirectional extru-

sion and crystallization takes place leading to the biogenesis of the  $\beta$  chitin whisker-like microfibrils.<sup>13,14</sup> To date no clear mechanism for the biogenesis of  $\alpha$  chitin microfibrils has been established despite the abundance of this allomorph in nature.

The solid state conversion of  $\beta$  chitin from the bristles of *Aphrodite* or *Palinurus* into  $\alpha$  chitin following intracrystalline swelling in concentrated nitric acid was first briefly described by Lotmar and Picken in 1950.<sup>4</sup> A few years later, Rudall<sup>11</sup> studied extensively the same phenomenon using concentrated HCl. He showed that the conversion was best observed with  $\beta$  chitin samples of low crystallinity such as those from squid pen. The conversion in HCl requires aqueous solutions of HCl with a strength of at least 6 N, but below 8.5 N since, at that concentration, HCl becomes a solvent for chitin.<sup>15</sup> In the solid state, the conversion  $\beta \rightarrow \alpha$  chitin frequently leads to a substantial shrinkage of the sample along its chain direction. This is, for instance, the case with squid pen for which a reduction of the pen length by about half results from the swelling treatment. To account for such shrinkage a chain-folding mechanism has been tentatively proposed by Rudall.<sup>11</sup> Such chain folding is well established in the case of flexible polymers as, for instance, polyethylene,<sup>16</sup> but it appears to be highly unlikely with polymer chains as stiff as those of chitin. Other possibilities can be invoked also, as in a given environment of  $\beta$  chitin, adjacent chitin microfibrils of both polarities may exist. Upon swelling, the chains of these up and down microfibrils could intermingle with the result of an interdigitation mechanism leading to a parallel ( $\beta$  chitin) to antiparallel ( $\alpha$  chitin) transformation that does not require a chain-folding process. In fact, such an interdigitation mechanism has been proposed to explain the mercerization of cellulose fibers<sup>17–20</sup> that match closely the solid state  $\beta \rightarrow \alpha$  transformation of chitin.

\* Author to whom correspondence should be addressed.

<sup>†</sup> CNRS.

<sup>‡</sup> University of Tokyo.

<sup>§</sup> Université Pierre et Marie Curie.

<sup>®</sup> Abstract published in *Advance ACS Abstracts*, May 1, 1997.

The present work was undertaken in order to clarify the molecular mechanism underlying the solid state swelling leading to the transformation  $\beta \rightarrow \alpha$  chitin. In particular, we were interested to see whether an interdigitation process similar to that accounted for in the mercerization of cellulose could be conceived to explain this transformation. The  $\beta \rightarrow \alpha$  chitin conversion was investigated with *Tevnia* chitin that is considered to be among one of the best crystalline  $\beta$  chitins.<sup>21</sup> Specimens of *Tevnia* were therefore subjected to swelling in aqueous HCl of various strengths, and the changes in their morphology and crystalline state were followed by transmission electron microscopy coupled with electron and X-ray diffraction together with FT-IR spectroscopy.

## Experimental Section

**Collection and Preparation of Purified  $\beta$  Chitin from *Tevnia*.** Tubes from *Tevnia jerichonana* were collected in November 1987 at a depth of 2600 m by the submersible Nautille during the Hydronaute cruise (A. M. Alayse-Danet and H. Felbeck chief scientists). The collection took place at a site located at 12°48' N, 103°56' W, near the Pacific rise. The wet tubes were dried and stored before being deproteinized following the method described earlier.<sup>21</sup> The resulting purified chitin microfibrils were dispersed by applying a hydrolysis step consisting in boiling them in 2.5 N HCl for 2 h. After thorough washing with distilled water, suspensions of these microfibrils were stored in 30% aqueous ethanol.

**Swelling in HCl.** All treatments were achieved at room temperature. Before HCl swelling treatment, the purified *Tevnia* chitin suspensions were washed 5 times by successive centrifugations in distilled water. Then one drop of concentrated sample suspension was added to a series of test tubes containing 10 mL of aqueous HCl of increasing concentration. After the swelling treatment that ranged from 30 min to 2 h, 100 mL of distilled water was added in order to deswell the samples. The specimens were then rinsed by centrifugation with distilled water until neutrality was reached. Some specimens were kept wet whereas others were dried.

The swelling of *Tevnia* chitin in concentrated HCl followed by washing created a substantial amount of amorphous material located at the surface of the samples. In order to visualize only the crystalline parts of the specimens, this amorphous material was removed in some of the samples by boiling the samples in 2.5 N aqueous HCl for 2 h.

**Transmission Electron Microscopy.** Drops of samples before and after treatment with HCl and washing in water were deposited on carbon-coated electron microscope grids. Some samples were negatively stained with uranyl sulfate whereas others were shadowed with W/Ta alloy. In addition unshadowed and unstained samples were also prepared.

Electron microscopy was achieved with a Philips CM200 CRYO transmission electron microscope (TEM) operated at 80 kV for imaging and 200 kV under low dose conditions for diffraction experiments.

**X-ray Diffraction Analysis.** All analyses were achieved with Warhus vacuum cameras fitted on a Philips PW 1720 X-ray generator operated with Ni-filtered Cu K $\alpha$  radiation. Powder patterns were obtained after freeze drying aqueous suspensions of the various specimens and mounting the dried samples into 1 mm thin walled X-ray capillaries. For  $\beta$  chitin, freeze drying resulted in the preparation of a mixture of chitin monohydrate and dihydrate. Anhydrous  $\beta$  chitin could be prepared by washing the samples in dry methanol and allowing them to dry in air at 50 °C. The  $\beta$  chitin dihydrate was prepared by refluxing the samples in 2.5 N HCl followed by washing overnight in water and squeezing out the excess water. For hydrated samples or those that were kept in acid, the specimens were sealed in 1 mm thin-walled capillaries before positioning in the vacuum X-ray camera. Calibration of the X-ray patterns was achieved with calcite (characteristic spacing, 0.3035 nm) dusted directly on the specimens or on the glass capillaries.

**FT-IR Measurements.** Suspensions of the samples, before and after swelling, were deposited into polyethylene caps in which they were allowed to dry in the form of thin films having thicknesses between 10 and 20  $\mu$ m. These films were dried under vacuum for 2 weeks at 50 °C and mounted across the 500  $\mu$ m hole of microdisk sample holders. These specimens were analyzed with a Fourier transform infrared (FT-IR) spectrometer, Perkin-Elmer Model 1720, equipped with a microfocus accessory which concentrates the infrared beam on a diameter of 1.5 mm. All spectra were recorded in transmission mode with an accumulation of 10 scans and a resolution of 4 cm<sup>-1</sup>.  $\alpha$  chitin standards were obtained from spectra of deproteinized crab tendons.

## Results

**1. Morphological Observations.** The solid state modifications brought by the swelling of *Tevnia* chitin in HCl were visualized by TEM. The initial samples of purified *Tevnia* chitin consisted of long smooth microfibrils with parallel edges. Their diameter varied from around 30 nm for the narrowest to 80 nm for the widest (Figures 1a and 2a). A treatment of these microfibrils with 7 N HCl for 30 min at room temperature followed by washing in water induced some structural modification that could be observed by TEM, after shadowing. This technique revealed that the surface of the microfibrils was no longer smooth but were covered with small slightly elongated protuberances (Figure 1b). By negative staining, other aspects of the structural modifications were revealed. Initially, the *Tevnia* microfibrils appeared featureless, with the exception of a few longitudinal striations (Figure 2a). After treatment for 30 min in 7 N HCl, each microfibril became subdivided into a series of smaller parallel elements no more than 2–3 nm in width (Figure 2b). A longer treatment in 7 N HCl induced more modifications of the chitin microfibrils. After a 2 h treatment, the microfibrils were still clearly visible but displayed numerous overgrowths organized in a more or less regular shish kebab type of organization (Figures 1c and 2c). In this sample, the "kebab" overgrowths reached 100 nm or even more in length for a width of the order of a few nanometers. Together with this feature, the subfibrillation of the core (the "shish") of the microfibrils was still clearly visible in the negatively stained samples. After a treatment in 8 N HCl for 30 min, the microfibrillar aspect of the *Tevnia* chitin was totally lost and the sample took the appearance of a gel. After washing in water, the gel structure yielded a consistent precipitate. By shadowing, it was found that this gel consisted of an assembly of tiny subelements each having lengths of around 50 nm (Figure 1d). After negative staining, it was found that the widths of these subelements were no more than 3 nm (Figure 2d).

**2. Crystallographic Data.** As the  $\beta$  chitin microfibrils from the vestimentiferan tubes are among the most crystalline samples of chitin, their swelling in HCl could be monitored easily by electron and X-ray diffraction techniques. A set of representative electron diffraction patterns is shown in Figure 3a–c. Parts a and b are both oriented with the chain axes  $c$  vertical whereas part c is an unoriented powder diagram. Part a corresponds to a pattern recorded on an individual initial chitin microfibril. This pattern consists of an array of spots that can be identified as the  $b^*c^*$  projection of the reciprocal lattice of  $\beta$  chitin.<sup>22</sup> In Figure 3b a similar pattern is shown, but recorded on a microfibril that had been treated for 30 min in 7 N HCl as in the cases of the samples imaged in Figures 1b and

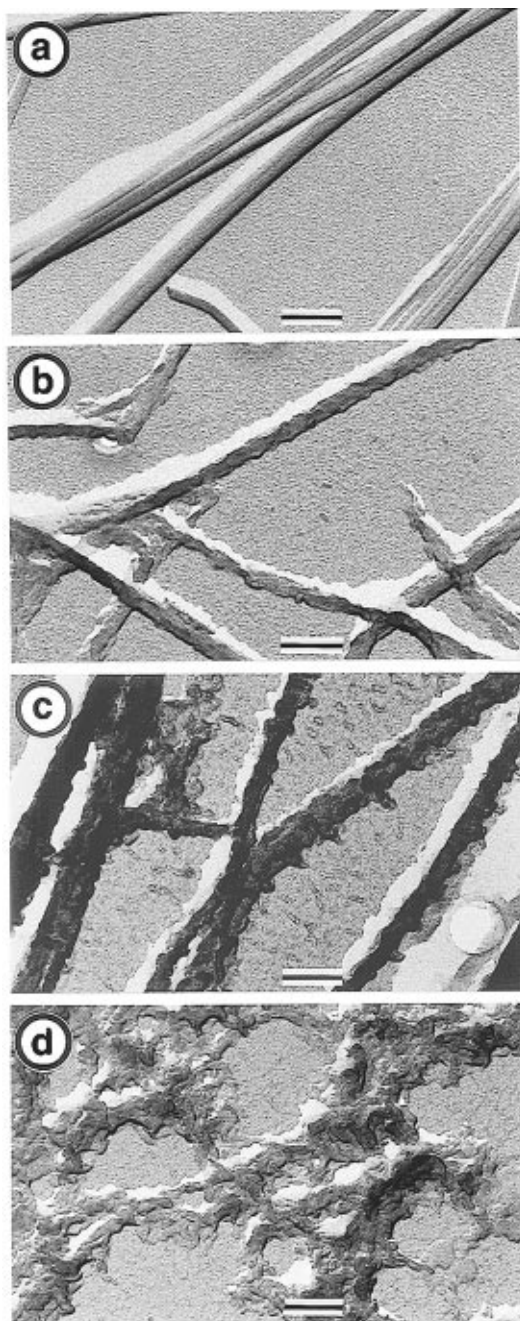


**Figure 1.** Set of shadowed electron micrographs describing the swelling of  $\beta$  chitin microfibrils from *T. jerichonana* into HCl. Scale bar = 200 nm. Key: (a) initial sample; (b) sample as in part a but after 30 min in 7 N HCl followed by washing in water; (c) sample as in part a but after 2 h in 7 N HCl followed by washing in water; (d) sample as in part a but after 30 min in 8 N HCl followed by washing in water.

2b. In addition this particular sample was also boiled in 2.5 N HCl for 2 h in order to remove the amorphous material created by the swelling action. The pattern in Figure 3b is similar to that in Figure 3a with the exception of a new reflection mirrored in the four equivalent weak spots (arrowed) on the third layer line. This new reflection that did not exist in the pattern of the initial sample is easily identified as the 013 ( $d = 0.338$  nm) of  $\alpha$  chitin.<sup>22</sup> With pure  $\alpha$  chitin, this reflection should be fairly strong. Its weakness in the pattern in Figure 3b indicates that the  $\alpha$  chitin component is minor in this composite diagram that is therefore a superposition of the  $b^*c^*$  projections of  $\alpha$  and  $\beta$  chitin. Remarkably, the two patterns of  $\alpha$  and  $\beta$  chitin are in

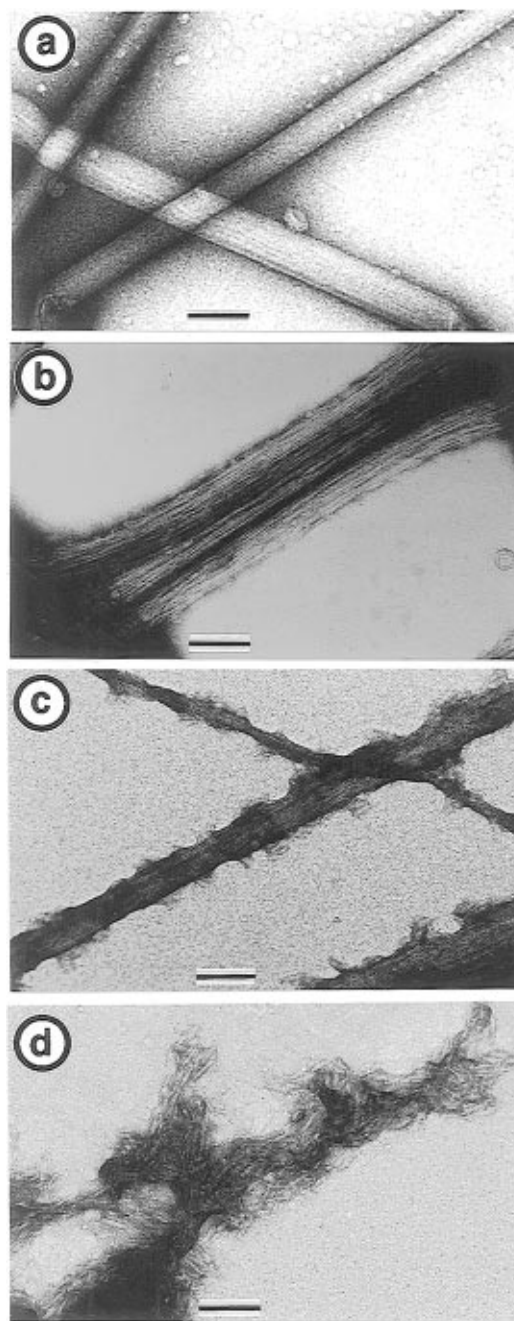


**Figure 2.** Set of negatively stained electron micrographs describing the swelling of  $\beta$  chitin microfibrils from *T. jerichonana* into HCl. Scale bar = 100 nm. Key: (a) initial sample; (b) sample as in part a but after 30 min in 7 N HCl followed by washing in water; (c) sample as in part a but after 2 h in 7 N HCl followed by washing in water; (d) sample as in part a but after 30 min in 8 N HCl followed by washing in water.

exact register along their  $b^*$  and  $c^*$  axes. Thus the  $\alpha$  chitin crystalline part is not only monocrystalline but is in epitactic association on the corresponding underlying  $\beta$  chitin crystal. The electron diffraction pattern in Figure 3c corresponds to a sample that was swollen in 8 N HCl for 30 min. This pattern, which is of the powder type consists of 2 strong rings calibrated at 0.474 and 0.338 nm. A third ring at around 0.94 nm was also observed sometimes but could not be reproduced by printing as it occurred in the inelastic background of the electron diffraction patterns. The presence of these rings allows to identify the corresponding sample as being essentially made of  $\alpha$  chitin. In this sample all orientation is lost, as a powder pattern such as the one

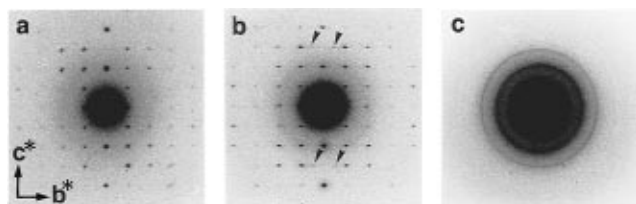


**Figure 3.** (a) Selected area electron diffraction diagrams on an isolated microfibril with vertical axis of initial *T. jerichonana* showing the typical  $b^*c^*$  projection of  $\beta$  chitin. (b) Same as part a but after immersion for 30 min in 7 N HCl, washing in water followed by 2 h boiling in 2.5 N HCl, and washing in water. The 013 strong diffraction spots of  $\alpha$  chitin are seen here as weak spots (arrowed). (c) Same as part a but after immersion for 30 min in 8 N HCl followed by washing. In this diagram, all orientation is lost and the diagram corresponds to  $\alpha$  chitin only.

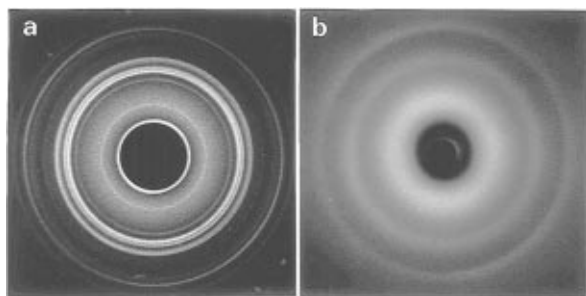


**Figure 4.** (a) X-ray diffraction pattern of initial *T. jerichonana*  $\beta$  chitin. (b) Same as in part a but kept in 6 N HCl.

shown in Figure 3c was uniformly observed throughout the specimen.

The swelling of *Tevnia* chitin was also followed by X-ray analysis achieved either in the acid swelling medium, after washing in water or after drying. Figure 4 illustrates the change in crystallinity occurring during the swelling in 6 N HCl. The diagram in Figure 4a corresponds to the initial sample in hydrated environment. This pattern is a typical well-resolved powder pattern of  $\beta$  chitin hydrate. The soaking of the sample in 6 N HCl (pattern in Figure 4b) induces a nearly total disappearance of the sharp rings seen in the pattern in 4a. This new diagram consists of only three rather broad peaks centered at 0.9, 0.45, and 0.34 nm. The peaks at 0.45 and 0.34 nm correspond roughly to the areas of maximum diffraction intensity in  $\beta$  chitin whereas the one at 0.9 can be assigned either to chitin or to the HCl which is soaking the sample. Remarkably, the transformation is reversible as upon washing in water; the pattern in Figure 4a could be restored with the exception that the inner ring occurred at a  $d$  spacing of 1.11 nm instead of 1.09 nm in the initial sample. Conversely, a new immersion into 6 N HCl gave again a pattern as in Figure 4b.

When the concentration of HCl was increased, the samples converted gradually to  $\alpha$  chitin. The occurrence of this polymorph is best detected by looking at the 0.9–1.2 nm area of the X-ray diagrams and the susceptibility of this region to hydration. Anhydrous  $\beta$  chitin possesses a strong 010 reflection at 0.924 nm. Upon hydration  $\beta$  chitin converts itself in a series of hydrates: a monohydrate where 010 takes the value of 1.04 nm and a dihydrate where 010 is increased to 1.16 nm.<sup>7</sup> Intermediate hydrates are also observed between the extreme values of 0.924 and 1.16 nm. A strong 020 reflection at 0.94 nm exists also in  $\alpha$  chitin. This reflection is insensitive to moisture uptake. Thus, by comparing the X-ray diagram of a given sample before

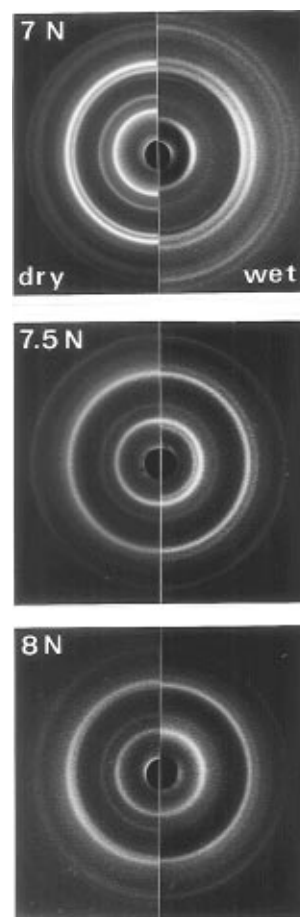


**Figure 5.** (a) X-ray diffraction pattern of a sample of *T. jerichonana*  $\beta$  chitin treated for 30 min in 7 N HCl followed by washing in water. Left: anhydrous sample. Right: sample moist with water. The inner ring is measured at 0.924 nm in the left as opposed to 1.123 nm in the right. (b) pattern as in part a but the sample was treated for 30 min in 7.5 N HCl. Left: anhydrous sample. Right: sample moist with water. The inner ring is measured at 0.932 nm in the left as opposed to a doublet at 0.932 and 1.099 nm in the right. (c) pattern as in part a but the sample was treated for 30 min in 8 N HCl. Left: anhydrous sample. Right: sample moist with water. The inner ring is measured at 0.920 nm in the left and is unchanged in the right.

and after a hydration treatment, one can detect easily the presence of  $\alpha$  chitin by looking at the 0.9/1.2 nm area of the X-ray diagrams. In Figure 5, a sample treated by 7 N HCl for 30 min did not show any noticeable presence of  $\alpha$  chitin as both its anhydrous or hydrated diffraction diagrams corresponded exactly to anhydrous  $\beta$  chitin and  $\beta$  chitin dihydrate. When the sample was kept for 30 min in 7.5 N HCl, a substantial amount of  $\alpha$  chitin was produced. The presence of this polymorph is clearly revealed in the hydrated sample where two reflections at 0.94 nm (020 of  $\alpha$  chitin) and 1.1 nm (010 of  $\beta$  chitin dihydrate) were seen. In this particular sample, the 0.94 nm reflection corresponding to  $\alpha$  chitin is much more intense than that at 1.1 nm of  $\beta$  chitin hydrate. In addition the other reflections, such as 0.33, 0.45, and 0.69 nm, were of  $\alpha$  chitin. Thus, this sample appears to contain more  $\alpha$  chitin than  $\beta$  chitin. When the sample was kept for 30 min in 8 N HCl, it was converted totally into  $\alpha$  chitin. This is revealed in the corresponding X-ray diagrams where the inner reflection at 0.94 nm remained unchanged when the sample went from an anhydrous state to a fully hydrated environment.

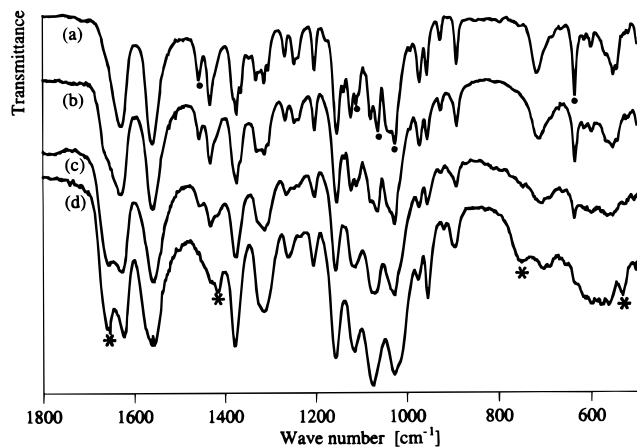


**Figure 6.** FT-IR spectra: (a) initial sample; (b) sample as in part a but after immersion in 6 N HCl for 30 min followed by washing and drying; (c) sample as in part b but the immersion was in 8 N HCl; (d) Specific IR spectrum of  $\alpha$  chitin from purified crab tendon. The black dots in the spectrum in part a correspond to absorption bands that are specific for the  $\beta$  allomorph of chitin. The stars in the spectrum in part d correspond to absorption bands that are specific for the  $\alpha$  allomorph of chitin.

**3. Spectroscopic Data.** The swelling of *Tevnia*  $\beta$  chitin was also followed by FT-IR. A set of representative spectra is shown in Figure 6. The initial sample gave a spectrum which corresponds to that of a high resolution spectrum of crystalline  $\beta$  chitin. As expected for such samples, there are two strong absorption bands in the C=O region, centered at 1630 and 1560  $\text{cm}^{-1}$ . In addition a number of specific absorption bands of  $\beta$  chitin that do not occur in  $\alpha$  chitin are identified with black dots in the spectrum. The spectrum in Figure 6b corresponds to a sample that was treated for 30 min in 6 N HCl. This spectrum presents a marked shoulder in the C=O region at around 1650  $\text{cm}^{-1}$ . In addition, the absorption bands that were identified with black dots in the spectrum in Figure 6a have lost some of their intensities. In the spectrum in Figure 6c from a sample immersed for 30 min in 8 N HCl, there are three absorption bands centered at 1655, 1627, and 1557  $\text{cm}^{-1}$  in the C=O region. In this spectrum, most of the bands identified with black dots in the spectrum in Figure 6a have either disappeared or are greatly diminished. The spectrum in Figure 6c is comparable to a spectrum of purified crab tendon chitin, known to consist exclusively of  $\alpha$  chitin and shown in Figure 6d. In this spectrum, the absorption bands that are specific of  $\alpha$  chitin are identified with stars.

## Discussion

The results obtained in this study present several interesting aspects of the interaction of aqueous HCl with crystalline  $\beta$  chitin. Up to a concentration of 6 N, the chitin from *T. jerichonana* remained unaffected when it was immersed in aqueous HCl as there was no apparent decrystallization or chitin solubilization. At a concentration of 6 N and above, HCl was able to swell the crystalline lattice of  $\beta$  chitin to yield a decrystallized HCl–chitin association showing only broad X-ray diffraction peaks (Figure 4b). Quite remarkably, if the concentration of HCl was maintained between 6 and 7 N, this decrystallization appeared to be reversible as the initial X-ray pattern of  $\beta$  chitin or one of its hydrates could not only be restored by washing in water but also no  $\alpha$  chitin could be detected in these patterns. By observation of these washed specimens by transmission

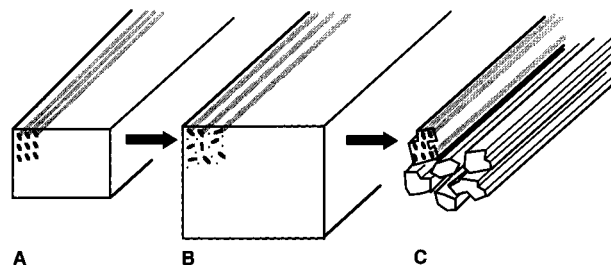


**Figure 7.** Schematic diagram describing the swelling of  $\beta$  chitin from *T. jerichonana* in 6–7 N HCl. Upon HCl uptake, the initial sample in part A undergoes an intracrystalline swelling without chain scission leading to a decrystallization as in part B. Upon washing in water, partial recrystallization occurs as in part C, leading to a subfibrillation of the chitin microfibrils. In this scheme, step C reverts entirely to  $\beta$  chitin. In part B of the drawing, the small dots represent the solvent molecules.

electron microscopy after negative staining, extensive longitudinal striations could be observed (Figure 2b). In the absence of images of sections of the corresponding samples, we could not ascertain whether these striations corresponded to surface grooves or whether they indicated real fractures of the microfibrils. In previous work, the sectioning of dried *Tevnia* chitin microfibrils revealed a number of cracking of the microfibrils under the stress of drying.<sup>21</sup> By similarity, we believe also that the striated structure seen in Figure 2b corresponds also to an extensive system of longitudinal cracks leading to a series of smaller parallel subfibrils. Thus, the apparent reversibility between the initial samples and those swollen in HCl existed only in terms of crystal structure but not in that of crystalline perfection. A schematic model of this reversible intracrystalline swelling is shown in Figure 7 where an initial microfibril in A becomes decrystallized with the uptake of aqueous HCl in B. This uptake induces a rupture of the intermolecular hydrogen bonds that hold the crystal together, but the long chains of chitin seem to remain parallel while keeping their length as the acid appears to be not strong enough to lead to substantial hydrolysis or dissolution. Upon being washed in water as in C, the chitin chains recrystallize in the initial  $\beta$  allomorph or one of its hydrates, but in doing so they yield a series of thinner parallel subfibrils as observed in Figure 2b.

When the  $\beta$  chitin from *T. jerichonana* was immersed in aqueous HCl of concentration ranging from 7 to 8 N, irreversible swelling occurred leading to some  $\alpha$  chitin which was observed after washing the samples in water. Remarkably, the  $\alpha$  chitin that was produced appeared to be deposited by epitaxy on top of the remaining microfibrillar  $\beta$  chitin to yield a shish kebab type of organization where the  $\alpha$  chitin part acted as “kebab” elements on top of the  $\beta$  chitin “shish”. A model of this irreversible swelling is shown in Figure 8 where an initial microfibril as in A is swollen in aqueous HCl of a normality comprised between 7 and 8 N. At this concentration the decrystallization is similar to that at 6 N, but some chain scission is believed to occur, yielding smaller chitin chains having significant mobility. It is these small chains that will recrystallize during washing in water to yield the shish kebab structure schematized in C.

As expected from the work of earlier workers,<sup>15</sup> the swelling of *T. jerichonana* chitin in aqueous HCl of normality 8 N and above led to a total conversion of  $\beta$  chitin into  $\alpha$  chitin. At the same time, the microfibrillar nature of the sample was completely lost (Figures 1d

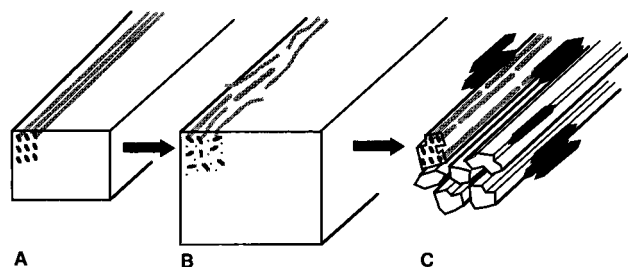


**Figure 8.** Schematic diagram describing the swelling of  $\beta$  chitin from *T. jerichonana* in 7.5–8 N HCl. Upon HCl uptake, the initial sample in part A undergoes an intracrystalline swelling together with chain scission leading to a decrystallization as in part B. Upon washing in water, partial recrystallization occurs as in part C, leading to a subfibrillation of the chitin microfibrils. In addition, the low molecular weight fragments that were partially solubilized in B will recrystallize in epitaxy on the surface of the chitin microfibril, leading to a typical "shish kebab" arrangement. In this drawing, the  $\alpha$  chitin crystals are shown as black spindle-like elements.

and 2d). This phenomenon is consistent with the effect of a joint action of dissolution and chain scission that is known to occur under these acid conditions.<sup>23</sup> The crystals of  $\alpha$  chitin that are viewed in Figures 1d and 2d correspond to spindle-like elements. Such morphology is classical in the case of chitin recrystallized from aqueous solution. It is in particular observed in *in vitro* chitin biosynthesis experiments.<sup>24–26</sup> In that case, it could be shown that the chitin chain axis was aligned with the long dimension of the crystals.<sup>25</sup>

In this work, we have followed the solid state transformation of isolated  $\beta$  chitin microfibrils made of parallel chains into a series of  $\alpha$  chitin crystals with antiparallel chains. The shish kebab mechanism which results from our observations accounts well for a gradual transformation of the parallel chain allomorph into the antiparallel one without losing the microfibrillar character of the initial sample. During the swelling treatment in HCl, the surface chains which are cut by the acid are unhinged from the underlying microfibrils and it is these chains that will recrystallize in an antiparallel mode on top of the remaining microfibrils in the subsequent washing treatment. Thus, it is only when all the sample has been solubilized with acid as strong as 8 N and above that all the microfibrillar morphology will be lost.

The  $\beta \rightarrow \alpha$  solid state transformation of chitin has been compared with the mercerization phenomenon of cellulose where the parallel chains of cellulose I are converted into the antiparallel structure of cellulose II. When isolated cellulose microfibrils from the highly crystalline samples such as those of *Valonia* were mercerized, a shish kebab mechanism similar to the one described here was seen.<sup>27,28</sup> This mechanism, however could not occur in the compact cell wall of *Valonia*<sup>29</sup> since there was no room for the growth of cellulose II lamellar crystals. For these cellulose samples, as well as those of cotton, ramie, flax, etc., an interdigitation mechanism of the cellulose chains from the up and down microfibrils has been invoked to explain the mercerization phenomenon.<sup>17–20</sup> In view of the similarity between the structure of  $\beta$  chitin and that of cellulose I, it is likely that an interdigitation mechanism may also have to be invoked in the case of the transformation  $\beta$  chitin  $\rightarrow$   $\alpha$  chitin for compact but less crystalline structures such as those of squid pen or *Aphrodite* bristles. If this was the case, a chain folding mechanism would not need to be invoked for the solid state conversion of these

specimens into  $\alpha$  chitin. It remains to be seen whether the  $\alpha$  chitin crystals resulting from the  $\beta \rightarrow \alpha$  transformation will consist of a perfect antiparallel arrangement or more likely of a statistical up and down arrangement.

The decrystallization of the large crystalline microfibrils of *Tevnia* chitin upon the action of acid and their subsequent recrystallization after washing is an interesting phenomenon that to our knowledge has not been much documented so far. In particular, if the acid strength is between 6 and 7 N, this treatment induces only a subfibrillation with no or only little conversion into  $\alpha$  chitin. This observation is reminiscent of a similar reversible intrafibrillar swelling observed with *Valonia* cellulose subjected to the interaction of liquid ammonia or anhydrous amines such as ethylenediamine.<sup>30–32</sup> As in the present work, the succession of intra-fibrillar swelling and de-swelling of cellulose induces a substantial subfibrillation clearly observed in negatively stained electron micrographs. With cellulose, the amine swelling treatments are known to increase drastically the accessibility and reactivity of cellulose toward chemicals.<sup>34,35</sup> In view of the similarity of the morphological changes resulting from the reversible intracrystalline swelling of cellulose and that observed with chitin in the present work, an increase in accessibility and reactivity should also be observed with  $\beta$  chitin after its swelling in acid of adequate strength.

Another aspect of the swelling of cellulose in ammonia or amines is that once the crystals are swollen, they can be washed in a number of solvents or chemicals that will stay as intercalates within the cellulose lattice.<sup>36</sup> In such a way, solvents such as chloroform, carbon tetrachloride, etc. can be incorporated in the crystalline lattice of cellulose. Such intercalates are also possible with  $\beta$  chitin. Their description and properties will be reported in the future.

**Acknowledgment.** Y.S. acknowledges the Centre de Recherches sur les Macromolécules Végétales (CERMAV-CNRS) for a 16 month fellowship. Part of this work was made as part of the DORSALES program and we acknowledge the financial help of the DRET (Grant 95-171).

## References and Notes

- (1) Blackwell, J. In *The Polysaccharides*; Walton, A. G., Eds.; Academic Press: New York and London, 1973; pp 464–513.
- (2) Roberts, G. A. F. In *Chitin Chemistry*; MacMillan Press: London, 1992; pp 21–35.
- (3) Muzzarelli, R. A. A. In *Chitin*; Pergamon Press: Oxford, England, and New York, 1977; pp 45–51.
- (4) Lotmar, W.; Picken, L. E. R. *Experientia* **1950**, *6*, 58.
- (5) Carlström, D. J. *Biophys. Biochem. Cytol.* **1957**, *3*, 669.
- (6) Minke, R.; Blackwell, J. *J. Mol. Biol.* **1978**, *120*, 167.
- (7) Blackwell, J. *Biopolymers* **1969**, *7*, 281.
- (8) Gardner, K.; Blackwell, J. *Biopolymers* **1975**, *14*, 1581.
- (9) Dweltz, N. E.; Colvin, J. R.; McInnes, A. G. *Can. J. Chem.* **1968**, *46*, 1513.
- (10) Dweltz, N. E. *Biochim. Biophys. Acta* **1961**, *51*, 283.
- (11) Rudall, K. M. *Adv. Insect Physiol.* **1963**, *1*, 257.
- (12) Rudall, K. M.; Kenchington, W. *Biol. Rev.* **1973**, *49*, 597.
- (13) Shillito, B.; Lübering, B.; Lechlaire, J.-P.; Childress, J. J.; Gaill, F. *J. Struct. Biol.* **1995**, *114*, 67.
- (14) Herth, W.; Barthlott, W. *J. Ultrastruct. Res.* **1979**, *68*, 6.
- (15) Clark, G. L.; Smith, A. F. *J. Phys. Chem.* **1936**, *40*, 863.
- (16) Wunderlich, B. in *Macromolecular Physics*; Academic Press: New York and London, 1973; Vol. 1, pp 267–275.
- (17) Okano, T.; Sarko, A. *J. Appl. Polym. Sci.* **1984**, *29*, 4175.
- (18) Okano, T.; Sarko, A. *J. Appl. Polym. Sci.* **1985**, *30*, 325.
- (19) Nishimura, H.; Sarko, A. *J. Appl. Polym. Sci.* **1987**, *33*, 855.
- (20) Nishimura, H.; Sarko, A. *J. Appl. Polym. Sci.* **1987**, *33*, 867.



- (21) Gaill, F.; Persson, J.; Sugiyama, J.; Vuong, R.; Chanzy, H. *J. Struct. Biol.* **1992**, *109*, 116.
- (22) Throughout this paper, we used for the anhydrous  $\beta$  chitin the monoclinic cell parameters  $a = 0.485$  nm,  $b = 0.926$  nm, and  $c$  (chain axis) = 1.038 nm,  $\gamma = 97.5^\circ$  as defined in ref 8. For the chitin hydrates, we used the parameters defined in ref 7. For  $\alpha$  chitin, we used the orthorhombic cell parameters  $a = 0.474$  nm,  $b = 1.886$  nm, and  $c$  (chain axis) = 1.032 nm as defined in ref 6.
- (23) Roberts, G. A. F. In *Chitin Chemistry*; MacMillan Press: London, 1992; pp 275–276.
- (24) Ruiz-Herrera, J.; Bartnicki-Garcia, S.; Bracker, C. E. *Biochim. Biophys. Acta* **1980**, *629*, 201.
- (25) Bartnicki-Garcia, S.; Persson, J.; Chanzy, H. *Arch. Biochem. Biophys.* **1994**, *310*, 6.
- (26) Fèvre, M.; Gay, L.; Chanzy, H. in *Modern Methods of Plant Analysis, Plant Cell Wall Analysis*; Linkens H. F., Jackson J. F., Eds.; Springer Verlag: Berlin and Heidelberg, Germany, 1996; Vol. 17, pp 88–89.
- (27) Chanzy, H. D.; Roche, E. J. *J. Polym. Sci., Polym. Phys Ed.* **1975**, *13*, 51.
- (28) Purz, H. J.; Fink, H. P. *Acta Polymerica* **1983**, *34*, 546.
- (29) Chanzy, H. D.; Roche, E. *J. Appl. Polym. Symp.* **1976**, *28*, 701.
- (30) Chanzy, H.; Henrissat, B.; Vuong, R.; Revol, J-F. *Holzforchung* **1986**, *40*, Suppl., 25.
- (31) Roche, E.; Chanzy, H. *Int. J. Biol. Macromol.* **1981**, *3*, 201.
- (32) Chanzy, H.; Henrissat, B.; Vincendon, M.; Tanner, S. T.; Belton, P. S. *Carbohydr. Res.* **1987**, *160*, 1.
- (33) Sugiyama, J.; Harada, H.; Saiki, H. *Int. J. Biol. Macromol.* **1987**, *20*, 122.
- (34) Herrick, F. W. *Appl. Polym. Symp.* **1983**, *37*, 993.
- (35) Schleicher, H.; Daniels, C.; Philipp, B. *J. Polym. Sci. Polym. Symp.* **1974**, *47*, 251.
- (36) Wade, R. H.; Creely, J. J. *Text. Res. J.* **1974**, *44*, 941.

MA961787+